Proceedings of the 11th ICPMG 2026
11th International Conference on Physical Modelling in Geotechnics
8-12 June 2026, Zurich, Switzerland

Effect of surcharge on geotextile tube on seepage control performance: a centrifuge modelling study

Chuanjin Tang*, Zhuofu Jiang, Jun Yuan Lee, Tse Shing Seah, Soon Hoe Chew
Department of Civil and Environmental Engineering, National University of Singapore, Singapore.

**chuanjin.tang@outlook.com*

ABSTRACT: This study investigates the influence of surcharge loading on the seepage control performance of a geotextile tube on top of an existing coastal structure under wave action. A newly developed physical modelling system in the Mark I geotechnical centrifuge at the National University of Singapore was employed. Initial test results indicate that applying a surcharge beyond a threshold value can significantly reduce seepage through the geotextile tube, whereas a surcharge of a much lower amount shows limited effectiveness. Further centrifuge tests are planned to improve the understanding of seepage control mechanisms in coastal geotextile tube applications.

1 INTRODUCTION

Sea-level rise induced by climate change poses significant threats to low-lying coastal regions and countries (e.g., Singapore). Existing coastal protection structures are primarily designed to withstand wave action. Additional features can be added to mitigate short-term sea-level rise associated with climate change; however, their capability to cut off seepage is often limited. Therefore, there is an urgent need to develop adaptable coastal protection structures to safeguard infrastructure and living spaces in coastal areas.

Large-scale on-site coastal protection experiments or observations often entail extremely long time and high financial costs. For instance, Xuan et al. (2022) reported a site investigation spanning more than ten years to evaluate the protective performance of various breakwaters (including geotubes) along the Mekong Delta, Vietnam. Finklenburg et al. (2024) conducted large-scale hydraulic model tests to study the effect of layout and filling materials of geotubes on failure mechanisms. Numerical simulations provide greater flexibility in reproducing diverse scenarios of coastal structure (Kim et al., 2015).

The centrifuge testing technique is a powerful tool in solving geotechnical engineering problems, owing to its capability of reproducing in-situ stress in small-scale models. Baba et al. (2002) studied the effect of different waves on coastal slopes using a drum centrifuge. Takahashi et al. (2019) developed a cam-type wave generator and carried out beam centrifuge tests of wave-coast interactions. Nevertheless, the studies on coastal protection structures through centrifuge modelling remain limited.

This paper presents a recent centrifuge modelling study on the effect of surcharge loading on the seepage control performance of a geotextile tube placed on top of a revetment. The paper first introduces a newly developed centrifuge model package, followed by preliminary results on wave actions and the corresponding responses of coastal structures and geotubes.

2 METHODOLOGY

2.1 Centrifuge model package

Figure 1(a) presents the centrifuge model package. The strongbox is composed of a transparent acrylic plate and aluminium plates, with an inner dimension of 750 mm × 300 mm × 260 mm. A thin rubber sealing layer was provided between the plates of the strongbox to prevent leakage.

The wave generation system comprised a motor, a linear guide rail, a vertical aluminium plate, and a control box. The motor was controlled by a Python program on a computer installed on the centrifuge and could drive the wave-generation plate in a reciprocating motion (with a maximum stroke of 300 mm) to generate waves. In this study, the wave-generation plate was set with a stroke of 40 mm and a period of 0.16 s.

The soil within the strongbox is Australia W9 sand supplied by Riversands Pty Ltd. It is a fine silica sand, with a nominal grain size of 0.1-0.5 mm, a D_{10} size of ~0.22 mm, a uniformity coefficient of <1.5, a specific gravity of 2.65, and maximum/minimum void ratios of 0.86/0.48 (Du et al., 2020).

Ultracompact pore water pressure (PWP) gauges, linear variable differential transformer (LVDT), radar, and high-speed cameras (see Figure 1(b)) were used to monitor and record the pore water pressure within the coastal structure, and the deformation/movement of the coastal structure and geotube under wave action.

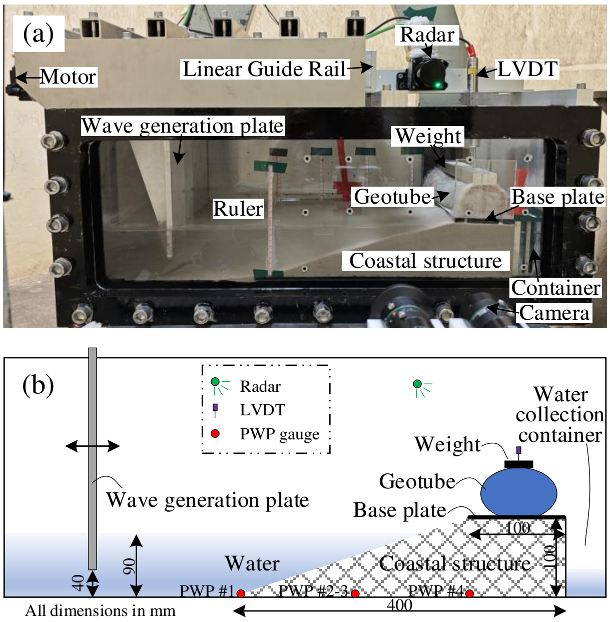

Figure 1. (a) Centrifuge model and (b) test layout with instrument.

2.2 Geotextile tube model

The geotextile tube model has an 80 mm-diameter, fabricated from 2 mm-thick nonwoven geotextile. It was infilled with a mixture: water: kaolin clay: cement at a mass ratio of 40:20:3. The geotube exhibited an approximately elliptical shape (with ~100 mm base width and ~50 mm height of the section) after being filled and stabilised (after 2-3 days).

2.3 Experiment setup

Figure 1(b) illustrates the test layout under plain strain conditions. The tests were conducted within the NUS Mark I centrifuge at 20 g (where g is gravity). The model represents a coastal profile with 90 mm water depth and a 100 mm high coastal structure. In prototype scale, it corresponds to a coastal section with a 1.8 m water depth, and a 2 m high coastal structure, on top of which there is a geotube with a 2 m base width and 1 m height. The model-scale and prototype-scale waves have the same Froude number Fr based on Eq. (1):

$$Fr = \frac{v}{\sqrt{Lg}} \quad (1)$$

where v is the velocity of the fluid flow (m/s), L is the characteristic length (m), and g is the gravitational acceleration (m/s^2).

2.4 Test plan

Table 1 summarises the four centrifuge tests to study the seepage control performance of geotubes under waves. Test GT-1 represents a standard geotube case; GT-2 and GT-4 indicate the cases where surcharge loads of 514 g and 1019 g are applied above a standard geotube; and GT-3 is the same configuration as GT-2 except that there was a plastic sheet covering the circumference of the geotube such that water could not pass through the geotube body. This configuration simulates the case when water could only pass through the interface between the geotube and the underlying acrylic base plate. This study focuses on two factors: (a) the effect of different surcharge loads (GT-1, GT-2, and GT-4), and (b) the effect of gaps between the geotube and the base plate (comparing GT-2 and GT-3). Note that the other parameters of the coastal structure and wave action were kept consistent for these four tests.

Table 1. Summary of test configuration (in model scale).

Test label	Plastic sheet covering geotube circumference	Surcharge load (g)	No. of waves upon test termination	Flow rate (ml/s)
GT-1	NIL	0	685	2.12
GT-2	NIL	514	719	3.62
GT-3	YES	514	754	2.18
GT-4	NIL	1019	506	1.51

2.5 Test procedures

The coastal structure model within the strongbox was prepared to achieve a relative sand density of 90% in dry status by a manually operated sand hopper (using the method reported in Tang et al. (2025)). The PWP gauges were installed at the base of the coastal structure after dry sand and subsequent water were till a certain depth, followed by installation of the remaining sand. The base plate was then placed on top of the coastal structure, where a geotube was placed. In tests GT-2, 3, and 4, additional weight was added onto the geotube to simulate vertical load.

After the centrifuge spun up to the target g-level, the in-flight wave generator was activated to generate waves with a frequency of 6.25 Hz. The experiment aimed to study the effects of 1000 waves on coastal structures and geotubes; however, the tests were terminated after 506-754 waves for different test configurations (see Table 1), which was based on the severity of wave erosion on the bottom of the acrylic base plate. The radar scanned the cross-sectional shapes of the geotube before wave generation and after wave cessation, and the cameras recorded the test process with images and videos.

3 TEST RESULTS

The results are presented in model scale.

3.1 Waveform

The wave-generation plate moved between positions w1, w2, w3, and back to w1 in a complete wave cycle, as shown in Figure 2. The water surfaces in these four photographs were depicted using blue dashed lines for easy identification.

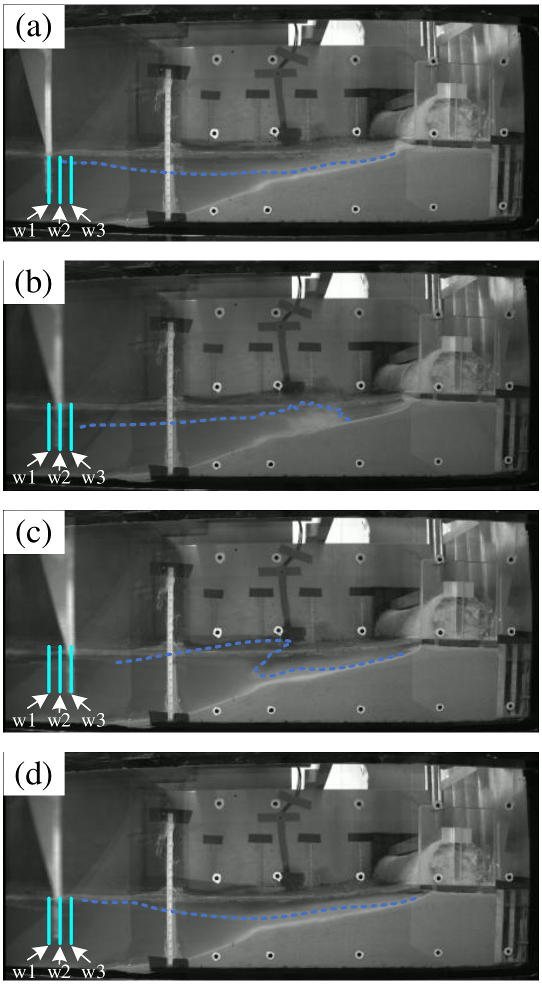

Figure 2. Observed waveforms in a complete cycle in test 2: wave-generation plate moving through positions at (a) w1, (b) w2, (c) w3, and back by (d) w2.

As the wave-generation plate moves from the w1 position towards the w2 position, it displaces water and generates an incident wave (from Figure 2 (a) to (b)), which propagates shoreward, breaks, and runs up the slope of the coastal structure. With continued plate motion towards the rightmost position (i.e. w3 position; Figure 2 (c)), the combined effects of continued plate-induced momentum and reflected/backflowing water from the coastal structure lead to a further increase in wave crest elevation. The resulting backwash entrains and transports sand seaward along the beach sloping face, leading to sediment redistribution characterised by a gentler upper swash slope and a comparatively steeper profile below the waterline. Takahashi et al. (2019) also reported a similar sand particle drift phenomenon near wave-breaking positions. Finally, as the wave-generation plate returns to the far-left position (i.e. w2 and w1 position; see Figure 2 (d) and (a)), the water is drawn back in the opposite direction, inducing a seaward-directed flow and a corresponding reduction in the nearshore water level.

Note that the present centrifuge setup is capable of generating only isolated transient waves rather than a continuous wave train at high *g* levels.

3.2 Water pressure

Figure 3 presents the selected water pressure time histories at PWP #1 (the location is shown in Figure 1(b)) of the four tests. The data presented correspond to waves No. 100-105.

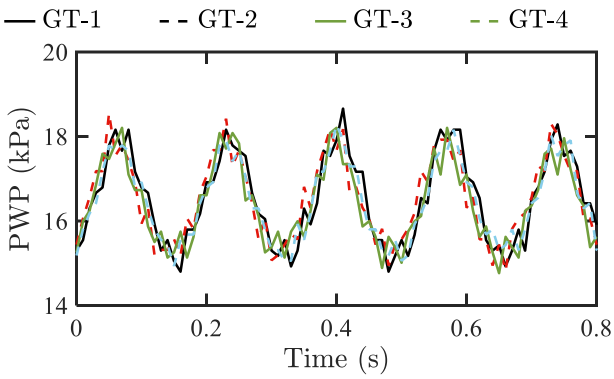

Figure 3. Water pressure at PWP #1.

The theoretically calculated hydrostatic pressure of PWP #1 is 16.4 kPa at the specific location. The measured water pressures across the different tests exhibit good repeatability, generally ranging between approximately 14.8-18.2 kPa, indicating a consistent wave-generation performance within a certain range. Similar repeatability was observed for PWP #2-4, while the responses of sensors at different locations reflected the spatial variation of wave action. As the wave generation process continued, the progressive sediment redistribution along the coast slopes became increasingly pronounced, which in turn influenced the local wave behaviour and sensor readings. This effect constitutes one of the reasons why the centrifuge tests were terminated after different numbers of waves for the various configurations, as summarised in Table 1.

3.3 Geotube anti-seepage performance

The interaction between waves and the geotextile tube mainly occurs as the wave-generation plate moved from the w2 position towards the w3 position (from Figure 2 (b) to (c)). During this stage, the wave run-up could reach approximately 20 mm above the base of the geotextile tube (which has an overall height of 50 mm). As the sides of the geotextile tube were sealed to the walls using silicone adhesive/tape, the transmitted water was constrained to pass through the geotextile tube itself and along the interface between the geotextile tube and the acrylic base plate. Water seepage through these pathways was collected in a container located on the landward side of the coastal structure, allowing the wave-blocking and seepage-control performance of the geotextile tube to be quantitatively evaluated under different test conditions.

The flow rates of different tests are summarised in Table 1. It was found that the seepage flow rate in test GT-3 (where there was a plastic sheet covering the geotube circumference) is lower than that in GT-2 (2.18 ml/s vs 3.62 ml/s). This difference is reasonable and as expected, because in GT-3, seepage predominantly occurred along the interface between the geotube and the base plate, while in GT-2, seepage happened both through the interface and the geotube body itself.

In tests GT-1, GT-2, and GT-4, the applied surcharge above the geotextile tube was 0 g, 514 g, and 1019 g, respectively, corresponding to approximately 0%, 42%, and 82% of the mass of the infill material (with the geotextile mass being negligible). Compared with the case without surcharge loads (GT-1), the application of a 42% surcharge (GT-2) resulted in a counterintuitive increase in seepage flow rate (2.12 ml/s vs 3.62 ml/s), since the additional surcharge loading would reduce the gap between the geotube and the base plate. This indicates a possible influence of experimental uncertainty. When comparing GT-1 and GT-4 (0 vs 82% in surcharge loads; 2.12 ml/s vs 1.51 ml/s in seepage flow rate) or comparing GT-2 and GT-4 (42% vs 82% in surcharge loads; 3.62 ml/s vs 1.51 ml/s in seepage flow rate), a clear reduction in seepage was observed under the effect of the additional vertical loads applied above the geotube.

4 CONCLUSIONS

This paper presents a centrifuge testing package for wave-coast interaction problems and investigates the effectiveness of geotextile tubes in controlling seepage. Initial testing results are provided, including the repeatability of wave actions and seepage behaviour of geotubes under different surcharge loading conditions. The paper offers a valuable methodological framework and data reference to support the assessment of geotextile tube-based coastal protection structures.

Future study will focus on coastal sloping face reinforcement, geotextile tube-base plate interaction, influence of geotube configuration and infill properties, as well as field tests, with the objective of establishing quantitative design parameters for practical geotextile tube-based coastal protection systems through scaling relationships derived from centrifuge modelling.

ACKNOWLEDGEMENTS

The authors are grateful to the National Research Foundation of Singapore, PUB (Singapore's National Water Agency) and National University of Singapore for supporting this work done in the Coastal Protection and Flood Resilience Institute (CFI) Singapore under the Coastal Protection and Flood Management Research Programme (CFRP) (2023/T1/V1-P2). The conclusions put forward in this publication reflect the views of the authors alone and not necessarily CFI Singapore or any of the supporting entities.

REFERENCES

Le Xuan, T., Ba, H. T., Thanh, V. Q., Wright, D. P., Tanim, A. H., and Anh, D. T. (2022). Evaluation of coastal protection strategies and proposing multiple lines of defense under climate change in the Mekong Delta for sustainable shoreline protection. *Ocean & Coastal Management*, 228:106301.

Finklenburg, B., Klopries, E. M., and Schuettrumpf, H. (2024). 2D failure mechanisms and failure modes of a new type of geotextile tubes used for river dikes. *Geotextiles and Geomembranes*, 52(4):690-703.

Kim, H. J., Won, M. S., and Jamin, J. C. (2015). Finite-element analysis on the stability of geotextile tube–reinforced embankments under scouring. *International Journal of Geomechanics*, 15(2):06014019.

Takahashi, H., Morikawa, Y. and Kashima, H. (2019). Centrifuge modelling of breaking waves and seashore ground. *International Journal of Physical Modelling in Geotechnics*, 19(3):115-127.

Baba, S., Miyake, M., Tsurugasaki, K. and Kim, H. (2002). Development of wave generation system in a drum centrifuge. *Proceedings of Physical Modelling in Geotechnics*, Phillips, R., Guo, P.J., and Popescu, R. (Eds.), St. John's, NL, Canada, pp. 265-270.

Du, S., Chian, S. C., and Qin, C. (2020). Post-liquefaction pore pressure dissipation in sand under cyclic stress triaxial testing. *Géotechnique*, 70(2):95-107.

Tang, C., Franza, A., Xu, J., and Marshall, A. M. (2025). Load transfer mechanisms for capped and uncapped non-displacement piles above tunnels: a centrifuge modelling study. *Géotechnique*, 75(4):550-562.